2^{nd} Workshop on CFD Uncertainty Analysis
October 19-20, 2006, Lisbon, Portugal

VERIFICATION OF VARIOUS MEASURES FOR NUMERICAL UNCERTAINTY USING MANUFACTURED SOLUTIONS

Francisco Elizalde-Blancas **Ismail B. Celik**

Mechanical and Aerospace Engineering Department, West Virginia University, Morgantown, WV, USA

ABSTRACT

In this study numerical solutions are presented for a steady state, incompressible, 2-D turbulent flow near a wall and over a backward facing step. For the case of turbulent flow near a wall a manufactured (exact) solution was provided by the organizers of the 2006 Lisbon Workshop [6]. With the help of manufactured solution, the true error and other relevant uncertainty measures are analyzed. The calculations were performed using the commercial flow solver FLUENT along with some user defined functions to define source terms and boundary conditions. A detailed grid convergence analysis was performed using four grid calculations and grouping them in triplets of possible combinations. The limiting values of the variables solved as the grid size tends to zero were calculated using different extrapolation methods. Based on this various numerical uncertainty estimates are presented followed by a comparative assessment.

1. INTRODUCTION

Numerical solutions of partial differential equations always entail errors from different sources. Two major sources of errors are modeling assumptions and the numerical methods. Error resulting from the numerical methods, known as numerical error, has been the subject of many recent studies [1, 2, 3, 4]. Various methods are available in literature to asses the numerical error in a given solution [1, 2, 3, 4]. However, since the exact solution is not known for a given problem it is very difficult to directly compare the performance of such methods in predicting the error itself. This problem was discussed during the Workshop on CFD Uncertainty Analysis in Lisbon, 2004. As a consequence, it was proposed to set up a manufactured solution that satisfies the continuity and momentum equations which can be used as an exact solution for error calculations. Such solutions are not obtained by analytically solving the governing equations but they are proposed solutions which satisfy the governing equations and exhibit the flow characteristics.

The objective of this study is to evaluate the performance of several extrapolation methods along with various uncertainty estimation methods in assessing the numerical uncertainty using a manufactured analytical solution. Then a methodology to assess the uncertainty is recommended and applied to case of flow over a backward facing step. The manufactured solution used is provided by the organizers of 2006 Lisbon Workshop [6]. Though the flow regime is turbulent; the numerical solution is carried out for pseudo-laminar flow in the case of flow near a wall (known exact solution). This was done in order to avoid the errors implicit in turbulence models. The transformation from turbulent to laminar flow was done by defining a momentum source term which precludes the pressure gradient term. Commercial flow solver FLUENT is used for numerical simulations with various grid densities. Also these numerical simulations were performed with 1^{st} and 2^{nd} order schemes for the convective terms. User Defined Functions (UDFs) were used to prescribe the sources and boundary conditions specified in the problem. Once the manufactured solution is known evaluation of several methods for quantification of numerical uncertainty such as Extrapolated Relative Error (ERE), Grid Convergence Index (GCI) and ERE_{cv2} [5] can be performed. Then it can be analyzed which of the methods used (combination of extrapolation and uncertainty quantification methods) better quantifies the numerical uncertainty

2. MANUFACTURED SOLUTION (MS)

The problem investigated in this study, has a manufactured solution which was provided by the organizers of the 2006 Lisbon Workshop [6, 9], . This manufactured solution satisfies identically the continuity equation and the momentum equation in the turbulent regime for an incompressible flow over a stationary wall where the computational domain is a square and delimited by $0.5\leq x\leq 1$ and $0\leq y\leq 0.5$, where x and y are dimensionless quantities.

The x-velocity component is given by

$$u = erf\,(\eta) \tag{1}$$

where the dimensionless variable η is given by

$$\eta = \frac{\sigma y}{x} \tag{2}$$

In Eq. (2) σ is a constant whose value used in this work is equal to 4.0.

The y- velocity component is given as follows

$$\upsilon = \frac{1}{\sigma\sqrt{\pi}}\left(1-e^{-\eta^2}\right) \tag{3}$$

While the pressure field is

$$C_p = \frac{P}{\rho U_{ref}^{\;2}} = 0.5\ln\left(2x-x^2+0.25\right)\ln\left(4y^3-3y^2+1.25\right) \tag{4}$$

Equations (1) to (4) represent dimensionless quantities but all the reference quantities were selected as unity. Therefore the dimensionless and dimensional quantities are equivalent.

3. MATHEMATICAL FORMULATIONS

Case with Manufactured Solution (MS)

The actual flow regime corresponds to a turbulent flow. However, as the principal objective of this work is to assess the numerical uncertainty, the error induced by the turbulence model was eliminated by modifying the equations as follows: The momentum equation in x direction is

$$\rho\left[u\frac{\partial u}{\partial x}+\upsilon\frac{\partial u}{\partial y}\right]=-\frac{\partial p}{\partial x}+\mu\left[\frac{\partial^2 u}{\partial x^2}+\frac{\partial^2 u}{\partial y^2}\right]+S_x \tag{5}$$

where S_x=0 for laminar flow but for turbulent flow it is given by

$$S_x=\frac{\partial}{\partial x}\left(\mu_t\frac{\partial u}{\partial x}\right)+\frac{\partial}{\partial y}\left(\mu_t\frac{\partial u}{\partial y}\right) \tag{6}$$

Similarly the momentum equation in y direction

$$\rho\left[u\frac{\partial \upsilon}{\partial x}+\upsilon\frac{\partial \upsilon}{\partial y}\right]=-\frac{\partial p}{\partial y}+\mu\left[\frac{\partial^2 \upsilon}{\partial x^2}+\frac{\partial^2 \upsilon}{\partial y^2}\right]+S_y \tag{7}$$

$$S_y=\frac{\partial}{\partial x}\left(\mu_t\frac{\partial \upsilon}{\partial x}\right)+\frac{\partial}{\partial y}\left(\mu_t\frac{\partial \upsilon}{\partial y}\right) \tag{8}$$

With the knowledge of the manufactured solution the source terms S_x and S_y can be calculated in terms of the flow variables u, v and p, giving

$$S_x=\left[-\frac{2\sigma\rho}{\sqrt{\pi}}\frac{y}{x^2}erf(\eta)+\frac{2\rho}{\pi}\left(\frac{1-e^{-\eta^2}}{x}\right)-\frac{4\mu\eta}{\sqrt{\pi}x^2}\left(1-\eta^2-\sigma^2\right)\right]e^{-\eta^2}$$
$$+\left(\frac{1-x}{2x-x^2+0.25}\right)\ln\left(4y^3-3y^2+1.25\right) \tag{9}$$

$$S_y=\left[-\frac{2\sigma\rho}{\sqrt{\pi}}\frac{y^2}{x^3}erf(\eta)+\frac{2\rho}{\pi}\frac{y}{x^2}\left(1-e^{-\eta^2}\right)\right]e^{-\eta^2}$$
$$-\left\{\frac{2\mu\sigma}{\sqrt{\pi}x^2}\left[\left(\frac{y}{x}\right)^2\left(3-2\eta^2\right)+\left(1-2\eta^2\right)\right]\right\}e^{-\eta^2}$$
$$+\frac{3y(2y-1)}{\left(4y^3-3y^2+1.25\right)}\ln\left(2x-x^2+0.25\right) \tag{10}$$

To check the pseudo-laminar model, the possible imbalance for the Navier-Stokes equations, was calculated for the manufactured solution in Eqs.(1-4) and resulted in the order of 10^{-17} which is negligible. Thus, in order to make the flow pseudo-laminar, the source terms S_x and S_y, Eqs. (9&10), are implemented in x- and y- momentum equations in FLUENT using UDFs.

Turbulence model for the Backward Facing Step (BFS)

As mentioned previously the flow regime for the BFS case is turbulent Re=5×10^4 with a reference velocity of 44.2 m/s. Here the Reynolds averaged Navier-Stokes (RANS) equations are solved along with a well known one equation Spalart-Allmaras turbulence model. This model solves a transport equation for the modified turbulent kinematic viscosity. The modified turbulent kinematic viscosity and the turbulent kinematic viscosity are identical except in the viscous affected region (near to the wall). The transport equation for the turbulent viscosity is given by

$$\frac{\partial}{\partial x_i}\left(\rho\bar{\nu}u_i\right)=G_\nu+\frac{1}{\sigma_{\bar{\nu}}}\left[\frac{\partial}{\partial x_j}\left\{\left(\mu+\rho\bar{\nu}\right)\frac{\partial\bar{\nu}}{\partial x_j}\right\}+C_{b2}\rho\left(\frac{\partial\bar{\nu}}{\partial x_j}\right)^2\right]-Y_\nu \tag{11a}$$

where the relation between the turbulent viscosity and modified kinematic viscosity is given by

$$\mu_t=\rho\bar{\nu}f_{\upsilon1} \tag{11b}$$

In Eq. (11a) $G_{\bar{\nu}}$ and $Y_{\bar{\nu}}$ are the production and destruction of turbulent viscosity respectively. The terms $\sigma_{\bar{\nu}}$ and C_{b2} are constants. For more details see [10].

The Spalart-Allmaras model was chosen to solve the flow over the BFS because it is a simple model and primarily because it was designed for applications involving wall-bounded flows.

4. NUMERICAL SETTINGS

Manufactured Solution Case

The computational domain for the MS is square 0.5≤ x≤ 1 and 0≤ y≤ 0.5. Except for the south (bottom) boundary, the boundary conditions prescribed were the analytical velocity profiles expressed in terms of x and y components. This was accomplished by making use of UDFs to evaluate Eqs. (1&3) at the boundaries. The south boundary was set as a wall with the no-slip condition.

To define the velocity profiles at appropriate boundaries, it is necessary to evaluate the error function in Eq. (1). The accurate evaluation of this function is critical to get good numerical results, particularly for the assessment of numerical uncertainty. In other words, the error induced by the evaluation of the error function must be as small as possible, in order to minimize its effect on predicted numerical uncertainty. At the beginning an equation with accuracy within 0.42 percent seemed to be good enough, however, it was not. Then a more accurate expression for evaluation was needed. The equation used is as follows

$$erf(\eta)=1-\left(a_1t+a_2t^2+a_3t^3+a_4t^4+a_5t^5\right)e^{-\eta^2}+\varepsilon(\eta)$$
$$t=\frac{1}{1+p\eta} \qquad |\varepsilon(\eta)|\le 1.5x10^{-7}$$
$$p=0.3275911 \qquad a_1=0.254829592$$
$$a_2=-0.284496736 \qquad a_3=1.421413741$$
$$a_4=-1.453152027 \qquad a_5=1.061405429 \tag{12}$$

In order to assess the numerical uncertainty several cases were run. The studied cases differ from each other in their grid density. Two sets of cases were defined as shown in Table 1. An orderly grid refinement was done between each case for every set. In each set the average grid size was decreased by a factor of four. For the particular case of (20x20) the solution did not converge satisfactorily, therefore a (19x19) grid was used. The coarsest grid was selected such that it was amenable to evaluate the performance of the extrapolation methods.

Case 1 of Set I corresponds to the coarsest grid and Case 4 for Set II represents the finest grid. Further finer grids were not considered because the interpolation error (bilinear method) was in the same order of magnitude as the true error, in which case the reliability in the assessment of the numerical uncertainty would be questionable.

Table 1 Cases studied for uncertainty assessment (MS).

Case	Set I	Set II
1	10x10	15x15
2	19x19	30x30
3	40x40	60x60
4	80x80	120x120

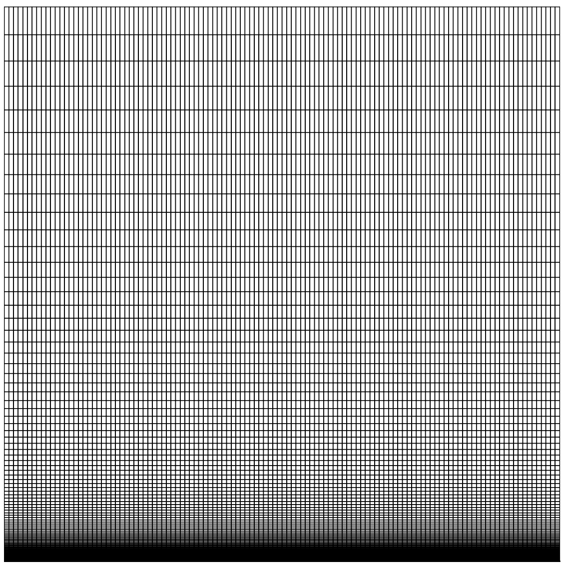

Figure 1. Grid characteristics for finest grid (MS).

The selected grids were structured, non-uniform with an expansion ratio of 0.95 in y-direction. The grid in y-direction is finer near the south boundary in order to predict, with reasonable accuracy, the velocity gradients inside the wall boundary layer. Along the x-direction the grid is uniform. A schematic view of the grid characteristics is shown in Fig. 1. The grid shown in this figure corresponds to the finest grid (Case 4, Set II).

All the cases shown in Table 1 were run with 1st and 2nd order upwinding schemes for the convective terms. However for uncertainty calculations only cases for Set I were considered.

Backward Facing Step (BFS)

In a similar way as in the manufactured solution case, use of UDFs to prescribe the boundary conditions were needed in the flow problem over the backward facing step. At the inlet of the backward facing step, profiles of *x*-velocity component and modified turbulent viscosity were prescribed. These inlet profiles were provided by the organizers of the 2006 Lisbon Workshop [6] as Fortran functions. At the outlet, pressure was set as atmospheric. The rest of the boundaries were treated as smooth walls (no roughness) with the no slip condition. The computational domain extends from -4H≤ X≤ 40H and 0≤ Y≤ 9H, where H is the height of the step (1.27 cm) and also the reference length. The origin of the coordinate system is located at the lower corner of the step and the height of the inlet section is 8H as shown in Fig. 2..

As mentioned before four grid calculations were utilized for uncertainty estimation. The grids used for the BFS consisted of 20774 cells for the finest grid (G1), 344 cells for the coarsest grid (G4). The medium grids have approximately 5146 cells (G2) and 1312 cells (G3). The refinement factor was 2 in both directions. The four grids were structured, uniform in *x*-direction and non-uniform in *y*-direction. Similar to the refinement factor the expansion ratio was not constant, varying in the range from 0.7 to 1.0 from coarsest to finest grid in different subregions. The grid is finer near the walls and in the shear layer region as depicted in Fig. 2.

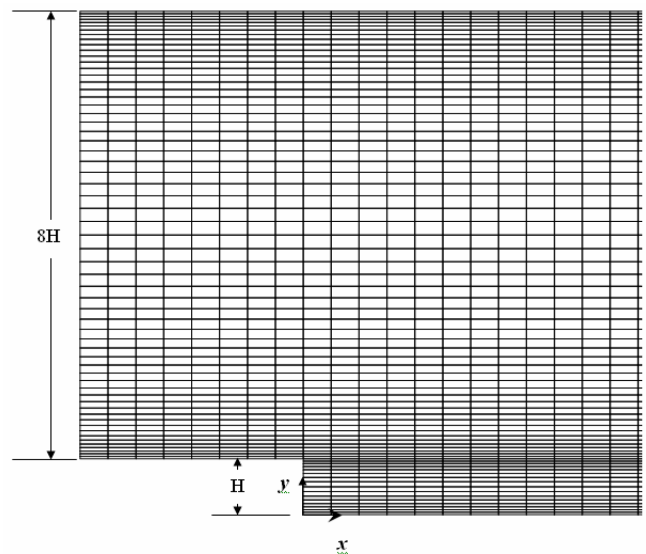

Figure 2. Grid characteristics for grid G2 (BFS).

5. METHODOLOGY FOR UNCERTAINTY ESTIMATION

With three grids (triplets from four grid calculations), extrapolation to zero grid cell size was performed with cubic spline, power law and AES extrapolation methods [5]. The average extrapolated value for each method is calculated by

$$\overline{\phi}_{ext} = \frac{\sum_{i=1}^{n} \phi_{ext}}{n} \tag{13}$$

where *n* is the number of possible triplet combinations from the four grid calculations (sample size). The standard deviation is calculated according to

$$\sigma = \sqrt{\frac{\left(\phi - \overline{\phi}_{ext}\right)^2}{n-1}} \tag{14}$$

and the coefficient of variance in the extrapolated values (CV_{ext}) as

$$CV_{ext} = \frac{\sigma}{\left|\overline{\phi}_{ext}\right|} \tag{15}$$

The extrapolated relative error (ERE) is used to quantify the uncertainty and it is evaluated by

$$ERE = \left| \frac{\phi_{ext} - \phi_f}{\phi_{ext}} \right| \quad (16)$$

and the extrapolated relative error considering the scatter in the extrapolated values defined as

$$ERE_{CV2} = ERE + CV_{ext} \quad (17)$$

One method to assess uncertainty is the fine grid convergence index (GCI) given by [7]

$$GCI = 1.25 \left| \frac{\phi_{ext} - \phi_f}{\phi_f} \right| \quad (18)$$

The term ϕ_{ext} in Eqs. (16&17) has two meanings. It is interpreted as the extrapolated value from the finest triplet (G1, G2, G3) and as the average extrapolated value as given by Eq. (13). Then, the first set of estimated uncertainties is given by

$$U_1 = \frac{\sum_{j=1}^{m} \left(\sum_{i=1}^{l} \left(ERE_i + ERE_{CV2,i} + GCI_i \right) \right)}{(mk)} \quad (19)$$

and the second set calculated as

$$U_2 = \frac{\sum_{j=1}^{m} \left(\sum_{i=1}^{l} \left(ERE_i + GCI_i \right) \right)}{(mk)} \quad (20)$$

where m equals 2 because of the two meanings of the extrapolated value, l equals the number of extrapolation methods considered and k is the product of number of extrapolation methods (three) times number of uncertainty estimation methods (three or two.) Therefore the statistics calculations considered to estimate U_1 and U_2 were based on 18 and 12 samples respectively. Finally, the uncertainties reported throughout this work are simply the average value of U_1 and U_2.

6. RESULTS

All the data presented in this work was obtained with first and second-order upwinding schemes (for convection) in the commercial flow solver FLUENT. The scheme applied to diffusion terms is second order central differencing. Double precision was used for all the calculations so that the round-off errors are minimized and thus can be considered negligible. The solution was considered a converged solution when scaled residuals were reduced to machine accuracy. The highest scaled residual for the MS case was in the order of 10^{-15} and for the BFS in the order of 10^{-10} for the second order scheme.

Case with Manufactured Solution

For all the cases shown in Table 1 the numerical solution was obtained and the true error was calculated using the manufactured solution. The manufactured solution contours are shown graphically in Fig. 3 along with the three flow variables. The velocity components, pressure and true error results for the finest grid case are shown in Figs. 4 and 5. Comparison of Fig. 4 with Fig. 3 shows that the qualitative and quantitative behaviors are very similar. The quantitative similarity can be better assessed when the true error is calculated. Fig. 5 presents the true error for the three flow variables. It can be seen from Fig. 5 that the absolute true error for all the flow variables is in order of 10^{-3} in most of the computational domain, and the highest true error is present near the east boundary.

In order to check the consistency of the numerical results, the calculated error at a single point is plotted against the non-dimensional average grid size in Fig. 6. The average grid size is calculated as $h = (A/N_{cells})^{1/2}$, where A represents the area of the computational domain and N_{cells} is the total number of cells in the domain. Hence, h_{max} corresponds to the average grid size for the coarsest grid. As can be seen in Fig. 6 the three flow variables show a convergence trend, meaning that for all the flow variables the true error is approaching zero as the grid size tends to zero.

A detailed post-processing of the data obtained from all the numerical solutions was done in order to assess the numerical uncertainty and the performance of several extrapolation methods. The post-processing consisted of selecting four different locations along x-direction inside the calculation domain to study the error behavior at these locations. These locations coincided with the cell centers for the coarsest grid and hence the cell center values were directly used. For finer grids, however, these locations fell in between the cell centers. Bilinear interpolation method was used to interpolate the cell center values for such grids at the exact locations of the cell centers corresponding to the coarsest grid.

Extrapolation to zero grid size was done making use of the power law method, polynomial method, cubic spline method and the Approximate Error Spline method (AES) proposed by Celik *et al.*[1].For a detailed description of these methods see [1]. The data required to calculate the extrapolated values of the flow variables was grouped in triplets for all possible combinations in each set of cases studied. The L_2 norm was calculated for the four locations (profiles) considered inside the computational domain according to the relation

$$L_2 = \sqrt{\frac{\left(\sum E_t^2\right)}{N_p}} \quad (20)$$

where E_t represents the true error and N_p the number of points on which the L_2 norm is calculated. The order of magnitude of the L_2 norm for both sets of groups is in the order of 10^{-4}. The computed values are shown in Tables 2 and 3 for sets I and II respectively.

Table 2. L_2 norm of true error for Set I

	u	**v**	**p**
Power law	1.095E-03	3.550E-04	1.106E-04
Cubic spline	6.319E-04	3.734E-04	1.163E-04
Polynomial	6.983E-04	5.560E-04	1.282E-04
AES	1.021E-03	2.732E-04	2.206E-04

Table 3. L_2 norm of true error for Set II

	u	**v**	**p**
Power law	5.059E-04	1.519E-04	1.378E-04
Cubic spline	4.708E-04	1.289E-04	1.156E-04
Polynomial	4.784E-04	2.195E-04	1.443E-04
AES	8.413E-04	2.695E-04	3.983E-04

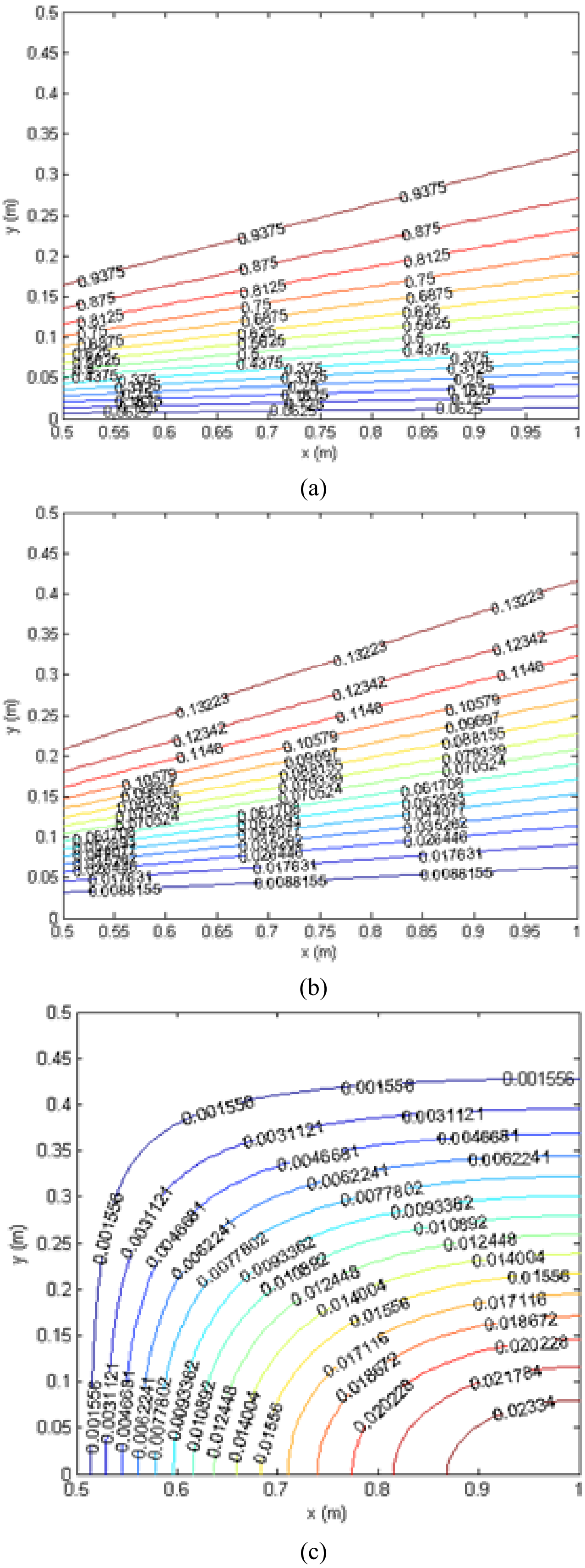

Figure 3. Flow variables distribution from manufactured solution; (a) velocity in x-direction, (b) velocity in y-direction, and (c) pressure.

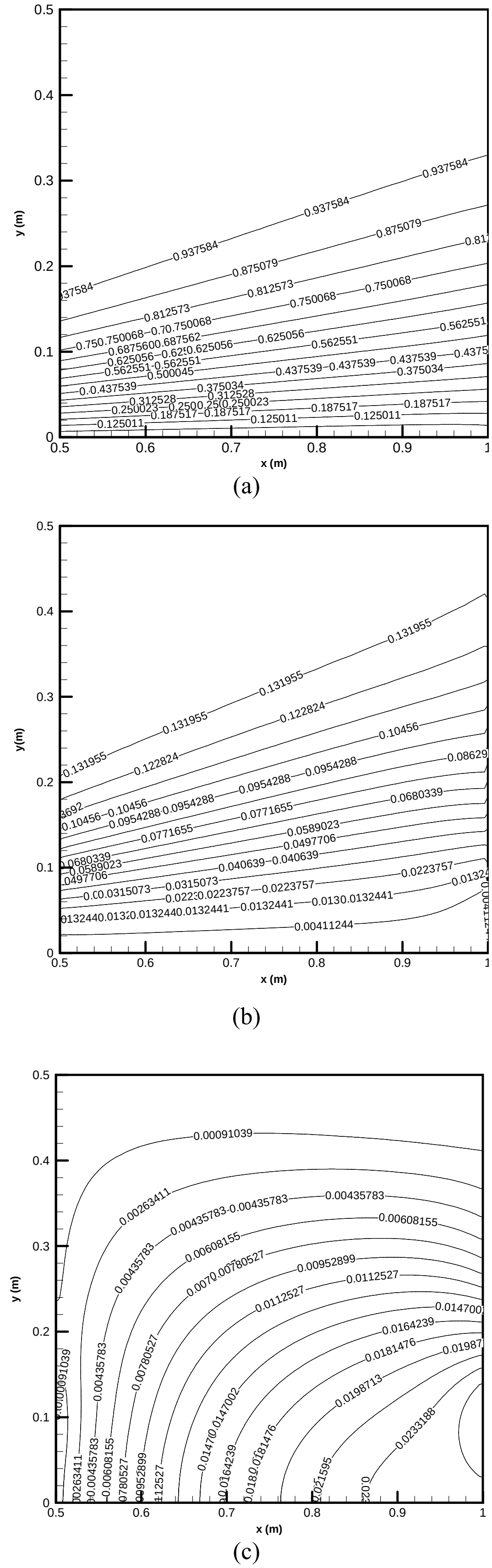

Figure 4 Numerical solution using FLUENT for the finest grid case; (a) x-velocity, (b) y-velocity, (c) pressure.

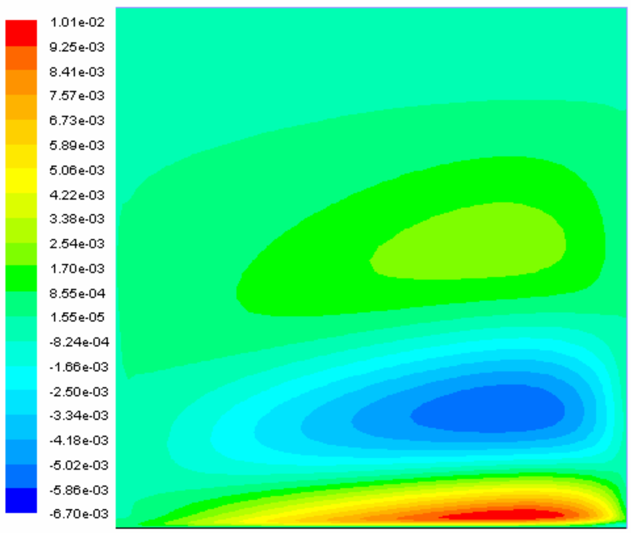

(a)

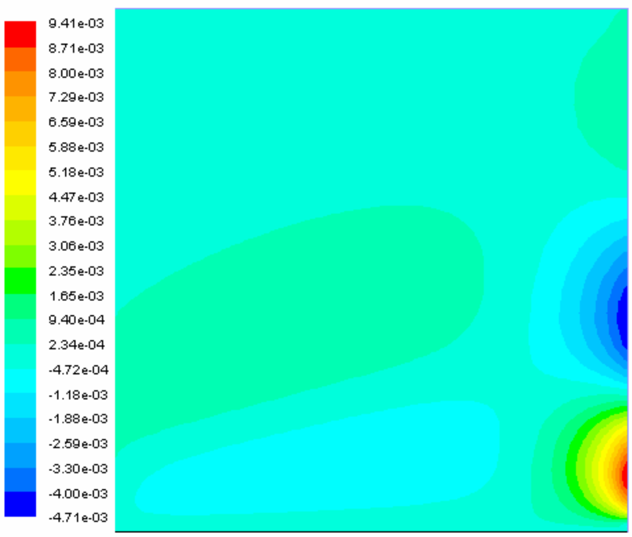

(b)

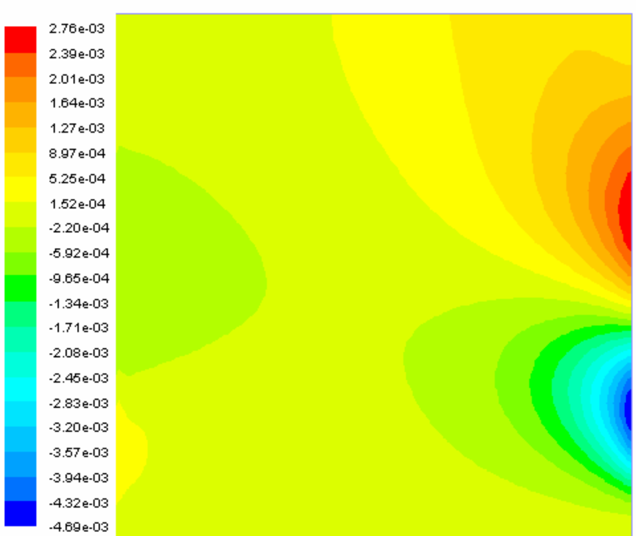

(c)

Figure 5 True error for finest grid case; (a) x-velocity, (b) y-velocity, (c) pressure.

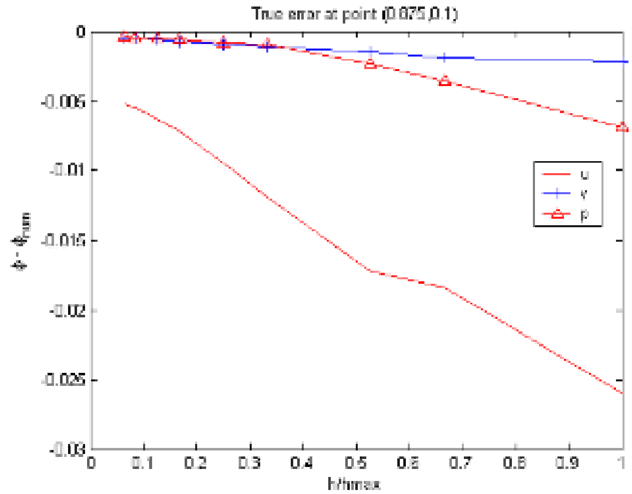

Figure 6 Grid convergence trends for the flow variables. Φ and Φ_{num} represent the true and numerical value of the flow variable respectively.

In Figs. 7 and 8 the normalized L_2 norm is presented for set I and set II respectively. For the first set, the extrapolation method that performs the best is the cubic spline among the four methods tested. For Set II the power law and cubic spline methods are both good but the cubic spline method performs better than the power law method. Considering both sets at the same time, the cubic spline method is judged as the best extrapolation method of the four methods analyzed in this work.

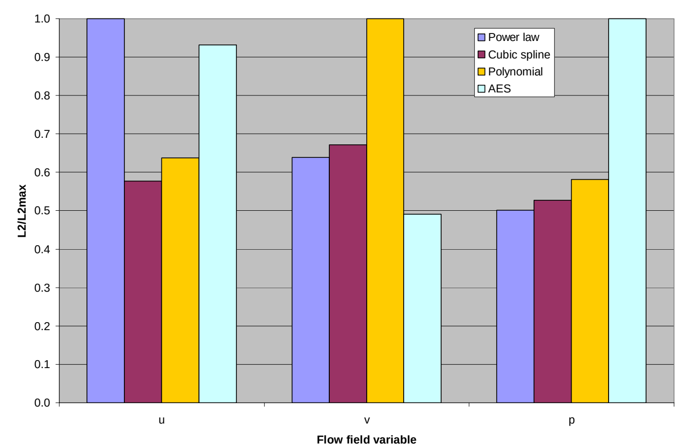

Figure 7 Normalized uncertainty for triplet combinations between cases of set I in Table 1.

Uncertainties of local flow quantities were estimated at three locations (x, y): (0.6, 0.001), (0.75, 0.002) and (0.9, 0.2). These uncertainties were calculated for first and second order schemes for u, v and C_p. The results are shown in Tables 4 & 5 for first and second order schemes respectively. Comparing data from Tables 4 & 5, uncertainty for second order solutions are smaller except for the pressure coefficient. Estimated uncertainties for v-velocity at first and second point are high because of the small predicted value for that variable. This behavior is explained by Eqs. 15 through 18. As the exact solution is known, the true uncertainty can be calculated and compared with the estimated uncertainties. This comparison is shown in Tables 6 and 7. From these tables it can be seen that the estimated uncertainties always over estimate the true uncertainty. The difference between 1st and 2nd order schemes is that the estimated uncertainty with second order is closer to the exact uncertainty than the first order.

Table 4 Predicted and uncertainty values of local flow variables for first order scheme (MS) *

Variable	**x=0.6,y=0.001**	**x=0.75,y=0.002**	**x=0.9, y=0.2**
u	5.8609E-3	7.5754E-3	7.9140E-1
Uncertainty u (%)	25.07 (± 1.469E-3)	74.94 (± 5.677E-3)	0.09 (± 7.122E-4)
v	1.2876E-5	2.0205E-5	7.7535E-2
Uncertainty v (%)	963.73 (± 1.24E-4)	4290.86 (± 8.626E-4)	0.44 (± 3.411E-4)
C_p	9.6480E-3	1.9294E-2	1.6763E-2
Uncertainty C_p (%)	1.66 (± 1.601E-4)	1.03 (± 1.987E-4)	0.62 (± 1.039E-4)

***** Values in parentheses indicate the actual error in that variable. The same notation is used in all of the tables given below.

Table 5 Predicted and uncertainty values of local flow variables for second order scheme (MS)

Variable	**x=0.6,y=0.001**	**x=0.75,y=0.002**	**x=0.9, y=0.2**
u	7.5327E-3	1.2140E-2	7.9101E-1
Uncertainty u (%)	2.23 (± 1.679E-3)	0.49 (± 5.948E-5)	0.03 (± 2.373E-4)
v	7.2024E-6	1.7572E-5	7.7019E-2
Uncertainty v (%)	445.4 (± 3.208E-5)	302 (± 5.306E-5)	0.08 (± 6.161E-5)
C_p	9.3950E-3	1.8950E-2	1.5877E-2
Uncertainty C_p (%)	2.17 (± 2.038E-4)	1.11 (± 2.103E-4)	1.42 (± 2.254E-4)

Table 6 Comparison between exact (μ) and estimated uncertainties for 1st order scheme (MS)

	x=0.6, y=0.001		**x=0.75, y=0.002**		**x=0.9, y=0.2**	
	μ	**estimated**	**μ**	**estimated**	**μ**	**estimated**
u (%)	22.09	25.07	37.06	74.94	0.02	0.09
v (%)	105.40	963.73	25.91	4290.86	0.64	0.44
Cp (%)	0.34	1.66	0.63	1.03	3.80	0.62

Table 7 Comparison between exact (μ) and estimated uncertainties for 2nd order scheme (MS)

	x=0.6, y=0.001		**x=0.75, y=0.002**		**x=0.9, y=0.2**	
	μ	**estimated**	**μ**	**estimated**	**μ**	**estimated**
u (%)	0.14	2.23	0.87	0.49	0.03	0.03
v (%)	14.90	445.48	9.50	302.00	0.03	0.08
Cp (%)	2.29	2.17	1.16	1.11	1.68	1.42

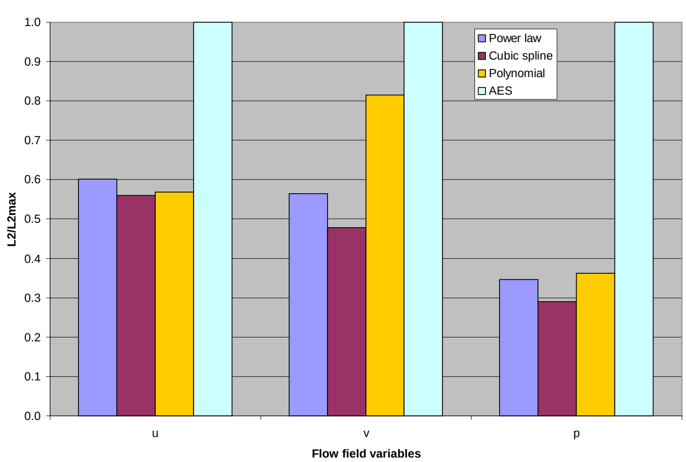

Figure 8 Normalized uncertainty for triplet combinations between cases of set II in Table 1.

The uncertainty for friction resistance coefficient at bottom wall is reported in Table 8. As expected the uncertainty for second order solution is much smaller than that for the first order.

Table 8 Predicted and uncertainty values of friction resistance coefficient at bottom wall.

	Predicted	**Uncertainty (%)**
First order	2.2999E-06	35.45 (± 8.153E-7)
Second order	3.2463E-06	1.46 (± 4.7396-8)

For the calculation of the overall friction resistance coefficient (integral quantities) the trapezoidal rule was the selected integration method.

The iteration error for all these calculations is estimated to be negligible as shown in Fig. 9, since the converged value practically is not changing at all after 80 iterations. When the iterative relative error is calculated it is in the order of 10^{-16}.

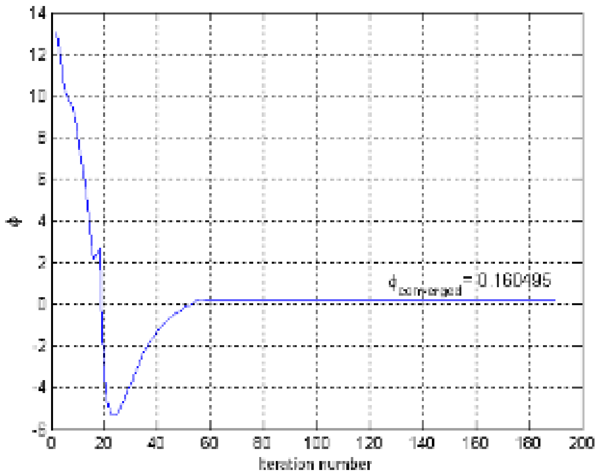

Figure 9 Behavior of *x*-velocity component as function of the iteration number.

In the results shown in Fig. 9 there is no interpolation error since the data correspond to the cell center of the nearby point to x=0.6, y=0.001 for a 1st order upwind. This corresponds to Case 4 Set I described in Table 1.

On the other hand, the interpolation error is always present and it could be eliminated only if the grid were manipulated in such a way that the reported points for every grid are located at the cell center.

Backward Facing Step

Uncertainty calculations for the backward facing step were focused at three points of interest. The locations of these points are (*x, y*): (0, 1.1H), (H, 0.1H) and, (4H, 0.1H). Uncertainties were estimated on both velocity components, pressure coefficient, modified turbulent viscosity, re-attachment point, friction resistance coefficient at bottom and top walls and, pressure resistance coefficient at bottom wall. All these calculations were performed for 1st and 2nd order numerical solutions for the convective terms. In Tables 9 & 10 are presented the uncertainties for local flow variables with first and second order schemes respectively. Comparing Table 9 and 10 it can be seen that almost all of the cases shown the uncertainties for second order simulations are smaller than those for the first order scheme. These are expected results. Unfortunately, without knowledge of the true solution we are not in the position to establish which of these methods would yield better results. However, from results obtained for the case with MS it would be expected that uncertainties estimated from first order scheme be more conservative. Such a conclusion requires more flow problems with a manufactured solution to be tested in order to be accepted and demonstrated as a valid statement.

Table 9 Predicted and uncertainty values of local flow variables for 1st order scheme (BFS)

Variable	**x=0,y=1.1H**	**x=H,y=0.1H**	**x=4H,y=0.1H**
u	0.69837	-0.2193704	-0.06803701
Uncertainty u (%)	2.93 (± 2.0462E-2)	4.46 (± 9.7839E-3)	54.34 (± 3.69713E-2)
v	-0.00047	0.0136924	-0.01170795
Uncertainty v (%)	709.49 (± 3.3346E-3)	5.29 (± 7.2432E-4)	4.83 (± 5.6549E-4)
C_p	-0.197410979	-0.2559408	-0.06681666
Uncertainty C_p (%)	2.091 (± 4.12786E-3)	9.73 (± 2.4903E-2)	24.2 (± 1.61696E-2)
ν_t	1.497384E-3	1.3771E-3	2.20131E-3
Uncertainty ν_t (%)	124.38 (± 1.86244E-3)	9.87 (± 1.359E-4)	4.07 (± 8.95933e-5)

Table 10 Predicted and uncertainty values of local flow variables for 2nd order scheme (BFS)

Variable	**x=0,y=1.1H**	**x=H,y=0.1H**	**x=4H,y=0.1H**
u	0.700446	-0.1966764	-0.1107796
Uncertainty u (%)	2.41 (± 1.688E-02)	0.47 (± 9.2437E-04)	9.48 (± 1.0502E-02)
v	-0.00773	0.0223564	-0.0114692
Uncertainty v (%)	46.68 (± 3.608E-03)	31.61 (±7.0668E-03)	4.21 (± 4.8285E-04)
C_p	-0.19925	-0.2333627	-0.0918282
Uncertainty C_p (%)	2.02 (± 4.02485E-03)	2.45 (± 5.7173E-03)	2.7 (± 2.4793E-03)
ν_t	1.43E-3	1.2094E-3	2.2154E-3
Uncertainty ν_t (%)	17.35 (± 2.481E-04)	15.37 (± 1.8588E-04)	0.43 (± 9.52622E-06)

Table 11 Predicted and uncertainty values in resistance coefficients at walls for 1st order

Flow quantity	**Predicted**	**Uncertainty (%)**
Friction resistance bottom wall	2.1805E-02	7.98 (± 1.74E-03)
Friction resistance top wall	3.3164E-02	41.28 (± 1.369E-02)
Pressure resistance bottom wall	1.1080E-01	6.27 (± 6.947E-03)

Table 12 Predicted and uncertainty values in resistance coefficients at walls for 2nd order

Flow quantity	Predicted	Uncertainty (%)
Friction resistance bottom wall	2.2008E-02	7.32 (± 1.6109E-03)
Friction resistance top wall	3.2922E-02	39.56 (± 1.303E-02)
Pressure resistance bottom wall	1.0413E-01	2.4 (± 2.499E-03)

Similarly as in some local flow variables, the uncertainties for the integrated variables such as friction resistance coefficient and pressure resistance coefficient at walls are smaller for second order upwind solutions than those for the first order (see Tables 11 & 12). Different to the MS case, the numerical integration method used to calculate these coefficients was the midpoint rule.

Completely similar to the trends mentioned above, the uncertainty of the re-attachment point decreases fast from first order calculations to second order solutions as shown in Table 13. Two methods to estimate the re-attachment point were performed; namely first by detecting the location where the axial velocity at the first grid cell center is zero, second by locating the point at which the wall shear stress is zero. Both methods predicted practically the same value of the re-attachment point. The reported values were calculated with the first method. The cubic spline interpolation method was used to estimate the re-attachment point.

Table 13 Predicted and uncertainty values for the re-attachment point

	Predicted	Uncertainty (%)
First order	5.51486	10.04 % (± 0.55369)
Second order	5.95309	2.77 % (± 0.1649)

All the reported values throughout this work are dimensionless quantities. For more detailed information on the uncertainty calculations for the Manufactured Solution and the Backward Facing Step flow problems see [8].

7. CONCLUSIONS

The use of manufactured solutions, could be a very useful technique to assess the numerical uncertainty. However, it is desirable that the manufactured solution be expressed in terms of functions that can be evaluated in a simple way. In case this is not feasible, care must be taken during the evaluation of complex function to guarantee a meaningful numerical error evaluation.

The pseudo-laminar method proposed in this work is a new alternative to avoid complexities and resulting induced errors inherent to turbulence models. Unfortunately, this methodology is only suited when a manufactured solution is known.

In case of iterative solutions, iterations must be continued till the scaled residuals reduce to machine accuracy if possible. If this can not be accomplished iterative error must be estimated and check a position to make sure that incomplete iterations are not a significant source of error. This is the case in this work where the highest residuals are in the order of 10^{-10} for the second order backward facing step case.

Special attention is required to the interpolation method and the interpolation error. When the interpolation error is in the same order of magnitude as the true error, finer grids will not be representative of the true error since the interpolation error is comparable with the true error. Ideally, it would be desirable to use a higher order interpolation method compared to the discretization method being used.

Of the four extrapolation methods evaluated in this study, the extrapolation method that performs the best is the cubic spline method, however the AES method would be the recommended extrapolation method to be used when the particular application is critical and a conservative safety factor is desirable.

It is recommended to use U_1 (Eqn. 19, average of the samples containing AES, cubic spline and polynomial extrapolation methods along with ERE, ERE_{CV2}, GCI) when the estimates are required to be conservative and, to use U_2 (Eqn. 20) for less conservative calculations. Also for best practice (as reported in this study) it is suggested to use the average of U_1 and U_2.

In order to make a statement about the use of the methodology presented throughout this work, it is necessary to gain confidence on the uncertainty estimation. The only way to achieve that goal is by exercising on many more fluid flow problems with carefully designed manufactured solutions.

NOMENCLATURE

A	computational domain area
C_p	pressure coefficient
h	average grid cell size
H	step height
N_{cells}	number of cells in the computational domain
p	pressure
S_x	momentum source term in x direction
S_y	momentum source term in y direction
u	x-velocity component
U_{ref}	velocity reference
v	y-velocity component

Greek symbols

Φ	flow variable
Φ_{ext}	extrapolated flow variable
Φ_f	flow variable for the finest grid
$\overline{V}$	modified turbulent viscosity
μ	viscosity
μ_t	turbulent viscosity
ρ	density
σ	standard deviation

REFERENCES

[1] Celik I, Li J, Hu G, Shaffer C. "Limitations of Richardson extrapolation and some possible remedies". *ASME Journal of Fluids Engineering* 2005; **127**:795 –805.

[2] Celik I, Karatekin O. "Numerical experiments on application of Richardson extrapolation with nonuniform grids". *ASME Journal of Fluids Engineering* 1997; **119**:584 – 590.

[3] Roache PJ. "Verification and Validation in Computational Science and Engineering". *Hermosa Publisher: Albuquerque*, 1998.

[4] Eça L, Hoekstra M (eds). *Proceedings of the Workshop on CFD Uncertainty Analysis,* Lisbon, 21–22 October, 2004.

[5] Celik I, Li J. "Assessment of numerical uncertainty for the calculations of turbulent flow over a backward-facing step". *Int. Journal for Numerical Methods in Fluids,* 2005; **49**: 1015–1031.

[6] *Workshop on CFD Uncertainty Analysis*, held in Lisbon, October, 19th and 20th, 2006 at Instituto Superior Técnico.

[7] Roache, P. I. "Perspective: a method for uniform reporting of grid refinement studies". *ASME Journal of Fluids Engineering* 1994; **116**; 405-413.

[8] Elizalde-Blancas F., Celik I. B., "Verification of Various Measures for Numerical Uncertainty Using Manufactured Solutions: an iteration and grid convergence study". Report # MAE-IC06TR01, October 2006.

[9] Eça L, Hoekstra M., Hay A., Pelletier D. "On the Construction of Manufactured Solutions for One and Two-Equation Eddy-Viscosity Models". Submitted to *International Journal for Numerical Methods in Fluids*.

[10] FLUENT Inc. FLUENT 6.2 User's Guide, 2005.